Study of Transverse Energy Production in Heavy-ion collisions

M.Sc. THESIS

by
Jeevan Kumar Sahoo

DEPARTMENT OF PHYSICS
INDIAN INSTITUTE OF TECHNOLOGY INDORE
June 2021

Study of Transverse Energy Production in Heavy-ion collisions

A THESIS

Submitted in partial fulfillment of the requirements for the award of the degree of

Master of Science

by

Jeevan Kumar Sahoo

under the guidance of

Dr. Raghunath Sahoo

DEPARTMENT OF PHYSICS
INDIAN INSTITUTE OF TECHNOLOGY INDORE

June 2021

INDIAN INSTITUTE OF TECHNOLOGY INDORE
CANDIDATE'S DECLARATION

I hereby certify that the work which is being presented in the thesis entitled **Study of Transverse Energy Production in Heavy-ion collisions** in the partial fulfillment of the requirements for the award of the degree of **MASTER OF SCIENCE** and submitted in the **Department of Physics, Indian Institute of Technology Indore**, is an authentic record of my own work carried out during the time period from August 2020 to June 2021 under the supervision of Dr. Raghunath Sahoo, Associate Professor, Indian Institute of Technology Indore.

The matter presented in this thesis has not been submitted by me for the award of any other degree of this or any other institute.

Jeevankr Sahoo
15/06/21

Signature of the student with date

(Jeevan Kumar Sahoo)

This is to certify that the above statement made by the candidate is correct to the best of my knowledge.

15/06/21

Signature of the M.SC. Thesis
Supervisor(with date)
(Dr. Raghunath Sahoo)

Jeevan Kumar Sahoo has successfully given his M.Sc. Oral Examination held on **June 18, 2021**.

18.06.2021

Signature of Supervisor of M.Sc. thesis
Date:

24-06-2021

Convener, DPGC
Date:

Signature of PSPC Member 1
Date: 19/06/2021

Signature of PSPC Member 2
Date: 19/06/21

Acknowledgements

I would first like to thank my supervisor, Dr. Raghunath Sahoo, whose expertise was invaluable in formulating the research questions and methodology. Your insightful feedback pushed me to sharpen my thinking and brought my work to a higher level. I would also like to thank my PSPC committee members, Dr. Manavendra N. Mahato and Dr. Dipankar Das for their help and motivation. I would like to thank Neelkamal bhai and Suraj bhai for the stimulating discussions and wonderful support. And also, I would also like to thank all my lab mates for their continuous support and help to clear any physics related questions.

In addition, I would like to thank my parents for their wise counsel and sympathetic ear. You are always there for me. Finally, I could not have completed this dissertation without the support of my friends, who provided stimulating discussions as well as happy distractions to rest my mind outside of my research.

Dedicated to my family.

Abstract

Understanding the transverse energy production in heavy-ion collisions is of paramount importance, in order to characterize the produced system and ensure the minimum energy density requirement for the formation of a deconfined system of quarks and gluons, called Quark-Gluon Plasma (QGP). In this work, we have studied the transverse energy (E_T) distributions for Au-Au collisions at RHIC energies and fitted a two parameter gamma distribution function to centrality-wise E_T distributions. We clearly observe that the shape parameter (α) is centrality dependent but, it does not depend on center-of-mass energy of the colliding nuclei. However, the rate parameter (β) is energy dependent. β also shows very little variation when seen as a function of centrality. A comparative study of convolution and summation of centrality-wise E_T distributions is also performed. It is found that, the minimum-bias E_T distribution can be obtained from bin-wise summation of the individual centrality-wise E_T distributions.

Table of Contents

List of Figures

List of Tables

Chapter 1

Introduction

In particle physics, elementary particles are those, which do not have any substructure. To study the elementariness of a particle, we need to know the spatial resolution of the probe. If two particles are separated by a distance Δr, then it can just be resolved with resolution Δr. If the probing beam itself consists of point-like objects, then the resolution is limited by the de Broglie wavelength of these beam particles i.e $\lambda = h/p$, where p is the beam momentum and h is the Planck's constant. So to resolve the shorter de Broglie wavelength, we need high momentum beam [1].

The theory of strong interaction called as Quantum Chromodynamics (QCD) states that at extreme conditions i.e at very high temperature and energy density, a phase transition occurs from normal hadronic matter to a deconfined state of quarks and gluons, called as the Quark-Gluon Plasma (QGP) [2,3]. The extreme conditions of temperature and energy density for the formation of Quark-Gluon Plasma (QGP) phase are T = 150-160 MeV and ε = 0.4 - 1 GeV/fm^3 respectively [4]. For the first time, QGP was detected at the CERN laboratory in the year 2000. In heavy-ion collision experiments, nuclei collide at relativistic speeds by forming extreme conditions of very high temperature and energy density at the collision point.

The properties of the matter formed in heavy-ion collisions could be studied through the transverse energy and charged-particle multiplicity distributions. These two observables also describe the particle production mechanisms in heavy-ion collisions. The transverse energy and charged-particle production depend on the impact parameter (*i.e.* transverse distance between the centers of the colliding nuclei) and the collision geometry. The information on the initial entropy and its subsequent evolution in the hot and dense matter could be found from the charged-particle multiplicity [5].

1.1 Heavy-ion Collisions

According to the big-bang theory, it is believed that, just after a few microseconds of the big-bang, the universe was filled with a state of matter known as the QGP. Scientists were curious to understand the properties of QGP. One of the ways to study the QGP is through heavy-ion collisions in the laboratories at extreme conditions of high temperature and energy density. When the two Lorentz contracted nuclei collide with each other, then the overlapping region looks like an almond shaped and nuclei release a large fraction of energy into a tiny volume of a fire ball. This tiny volume of fire ball consists of quarks and gluons in a deconfined state. The created fire ball expands and cools down until the produced particles reach kinetic freeze-out. These collisions provide information about the global properties, particle production mechanisms and macroscopic properties of QGP. Figure 1.1 shows the schematic representation of heavy-ion collisions.

The first relativistic heavy-ion collision experiment was studied at Brookhaven and Super Proton Synchrotron (SPS) at the European Laboratory with the center of mass energies of 33 GeV and 400 GeV respectively in the 1970s and 80s. Now most of the experiments are performed at the Relativistic Heavy-Ion Collider (RHIC), BNL, USA and A Large Ion Collider Experiment (ALICE)

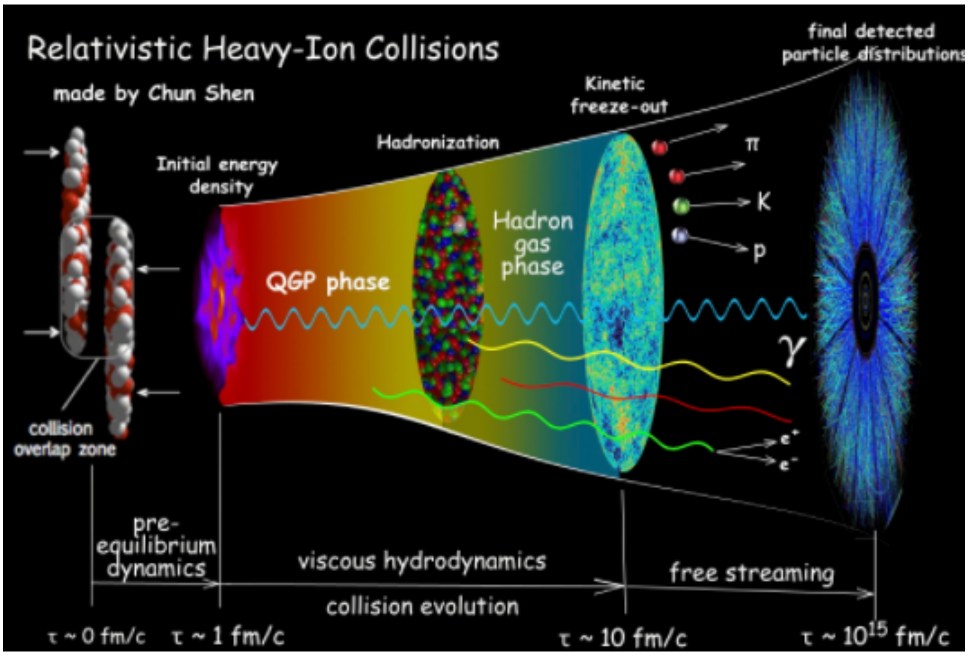

Figure 1.1: Relativistic heavy-ion collisions. (Source : Online)

detector at the Large Hadron Collider (LHC) at CERN, Switzerland [6].

1.2 QGP and Space time-evolution

Quark gluon plasma is the deconfined state of quarks and gluons. This state exists at very high temperatures and very high energy densities. It is believed that the whole universe is filled with QGP before any matter was created. This state of matter can also be produced in the laboratories by providing enough heat and pressure to the collisions, which is done at the RHIC and LHC energies. For the first time QGP was observed at CERN in the year of 2000.

In figure 1.2, the temperature is plotted against the net baryon density of the system. In this figure, high temperature and low baryon density corresponds to early universe that might have existed billions of years ago and the other one low temperature and high baryon density correspond to different astrophysical objects like neutron stars. The first order phase transition separates the decon-

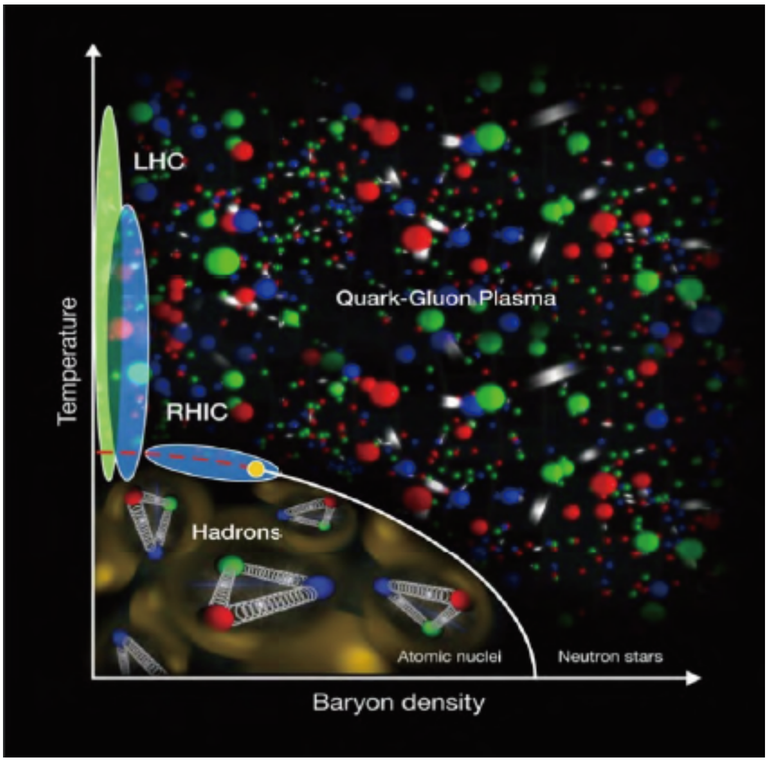

Figure 1.2: A schematic of the QCD phase diagram [7].

fined QGP from confined hadronic matter, which ends with a possible critical end-point (CP). So we observe a crossover transition in the RHIC and LHC energy regimes. The energy density and temperature required for such phase transition from deconfined QGP to confined hadronic matter is $\varepsilon_c = 1\ GeV/fm^3$ and $T_c = 150 - 170\ MeV$ respectively [8].

The space-time evolution in the hadronic and heavy-ion collisions are shown in figure 1.3, which are complex phenomena involving various degrees of freedom at different space-time coordinates. When two nuclei collide with each other, then a large amount of energy and temperature are produced in a tiny fireball. Initially in the system deconfined partons (quarks and gluons) are produced, called pre-equilibrium phase followed by a thermalised deconfined QGP medium and then a possible mixed phase occurs which should follow first order phase transition signatures. After that hadronization occurs, where composite hadrons are produced from quarks and gluons. The point at which possible phase transition occurs from deconfined QGP to hadron gas is called critical temperature

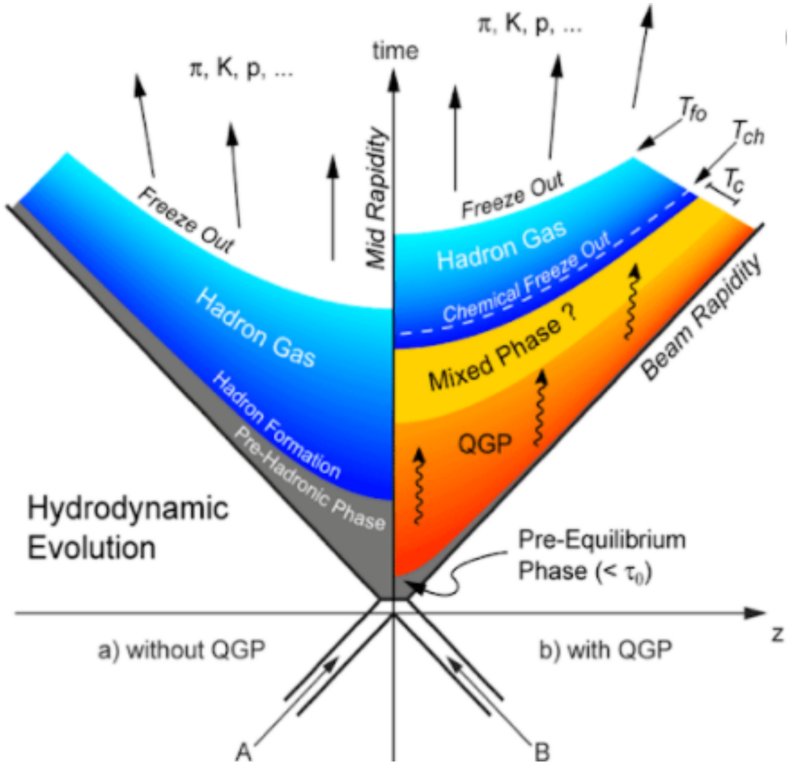

Figure 1.3: A schematic diagram space-time evolution in hadronic collisions, compared with heavy-ion collisions [7]).

(T_c). After that, chemical freeze-out occurs where inelastic collisions cease to exist. This is characterized by the chemical freeze-out temperature (T_{ch}) and the baryochemical potential (μ_B) of the system. The produced particles undergo inelastic collisions among themselves and exchange momentum. At a certain temperature known as the kinetic freeze-out (T_{fo}), as the mean free path of the particles becomes larger than system size, elastic collisions stops and particles move towards the detectors and get detected.

The left part of figure 1.3 represents the space-time evolution of collisions without QGP formation. Generally the low multiplicity pp collisions show this character. After the collision, the system goes through preequilibrium phase followed by chemical freeze-out without a QGP phase. After that produced hadrons attend kinetic freeze-out, and finally get detected by the detector.

1.3 Motivation

It is believed that a few microseconds after the Big Bang the whole universe was filled with a hot dense matter, called Quark-Gluon Plasma (QGP). Since the universe cooled down gradually, the quarks and gluons combined to produce hadrons such as protons and neutrons which are the building blocks of atoms of the elements. So it is important to study the early states of matter i.e. QGP, to understand the evolution of the universe from the beginning. Ultra-relativistic heavy-ion collisions produce this sate of matter for a very short duration. Observables like transverse energy and transverse momentum are crucial in such collisions. Transverse energy is related to the collision geometry. Since E_T production were the result of the creation of particles according to the semi-inclusive multiplicity distribution followed by the random assignment of transverse momentum to each particle, so the process would be described by the below equation,

$$\frac{d\sigma}{dE_T} = \sigma \sum_{n=1}^{n_{max}} f_{NBD}(n, 1/k, \mu) f_{\Gamma}(E_T, \alpha, \beta) \tag{1.1}$$

where f_{NBD} (negative binomial distribution) represents the multiplicity distribution of the collisions and f_{Γ} (gamma distribution) represents the E_T distribution of the particles. So to study the E_T production, one can fit gamma distribution function to centrality-wise E_T distribution curves [9].

In the next chapter we discuss some kinetmatic variables relevant to study the heavy-ion collisions. All the particles are treated as relativistic due to their speed being nearly close to the speed of light.

Chapter 2

Basic Kinematics

2.1 Rapidity

Since velocity is not an additive quantity in Lorentz boosted frames, so in successive transformations, velocity becomes non-linear and it is difficult to handle. So a new kinematic variable was introduced, called the rapidity. Rapidity is a dimensionless quantity and additive in successive transformations in boosted Lorentz frames. It is defined as,

$$y = \frac{1}{2} \ln \left(\frac{E + p_z}{E - p_z} \right) = \ln \left(\frac{E + p_z}{m_T} \right) \tag{2.1}$$

where, m_T is the transverse mass, defined as $m_T = \sqrt{m^2 + p_T^2}$, p_T is the transverse momentum, defined as $p_T = \sqrt{p_x^2 + p_y^2}$, p_z is the longitudinal momentum of the particle and E is the total energy of the particle, defined as $E = \sqrt{p_x^2 + p_y^2 + p_z^2 + m^2 c^4}$.

2.2 Pseudorapidity

When the particle is emitted at an angle θ from the primary vertex (point of collision), then the longitudinal momentum can be written as $p_z = |\vec{p}|\cos\theta$. Now the rapidity becomes,

$$y = \frac{1}{2}\ln\left(\frac{E + p_z c}{E - p_z c}\right)$$

$$= \frac{1}{2}\ln\left(\frac{\sqrt{p^2c^2 + m^2c^4} + p_z c}{\sqrt{p^2c^2 + m^2c^4} - p_z c}\right)$$

At higher energies $p^2c^2 >> m^2c^4$,

$$y = \frac{1}{2}\ln\left(\frac{pc\sqrt{1 + \frac{m^2c^4}{p^2c^2}} + p_z c}{pc\sqrt{1 + \frac{m^2c^4}{p^2c^2}} - p_z c}\right)$$

$$\approx \frac{1}{2}\ln\left(\frac{pc + p_z c + \frac{m^2c^4}{2pc} + \ldots}{pc - p_z c + \frac{m^2c^4}{2pc} + \ldots}\right)$$

$$\approx \frac{1}{2}\ln\left(\frac{1 + \frac{p_z}{p} + \frac{m^2c^4}{2p^2c^4} + \ldots}{1 - \frac{p_z}{p} + \frac{m^2c^4}{2p^2c^4} + \ldots}\right)$$

$$y \approx \frac{1}{2}\ln\left(\frac{1 + \cos\theta}{1 - \cos\theta}\right)$$

$$y \approx \eta = -\ln\left(\tan\frac{\theta}{2}\right) \tag{2.2}$$

Hence in ultra-relativistic domain, rapidity (y) is approximately same as the pseudorapidity (η).

The relation between rapidity and pseudorapidity is as follows,

$$\frac{dN}{d\eta} = \sqrt{1 - \frac{m^2}{m_T^2 + \cosh^2 y}}\frac{dN}{dy} \tag{2.3}$$

For massless particles both η and y are the same.

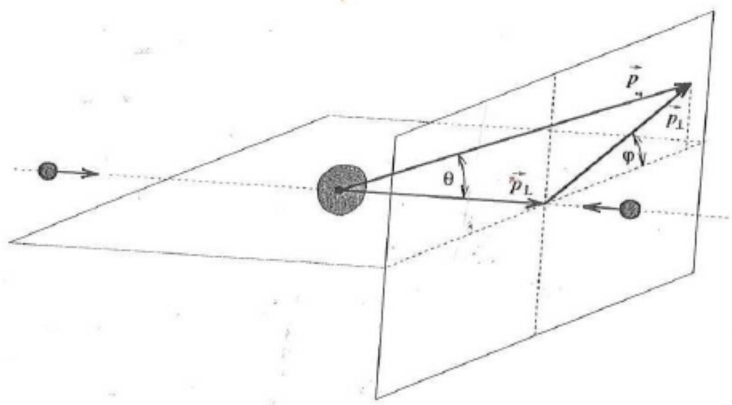

Figure 2.1: A schematic decomposition of detector co-ordinate system [1].

2.3 Detector co-ordinate system

A schematic representation of a detector co-ordinate system is shown in Fig 2.1. Here θ is the angle of inclination of $\vec{p}$ along beam axis and ϕ is the azimuthal angle. In collider experiments, particles could be tracked by having their momentum components (p_x, p_y, p_z). From their momentum components, θ, ϕ, p_T and η could be estimated.

$$\phi = \tan^{-1}(p_y/p_x) \tag{2.4}$$

$$\theta = \cos^{-1}(p_z/|\vec{p}|) \tag{2.5}$$

where p_z is called longitudinal momentum and $p_T = \sqrt{p_x^2 + p_y^2}$ is called transverse momentum.

$$y = \frac{1}{2}\ln\left(\frac{E+p_z}{E-p_z}\right) = \ln\left(\frac{E+p_z}{m_T}\right) \tag{2.6}$$

where m_T is the transverse mass, which is defined as $m_T = \sqrt{m^2 + p_T^2}$, m is the rest mass of the particle. In ultra-relativistic collisions, rapidity is approximated

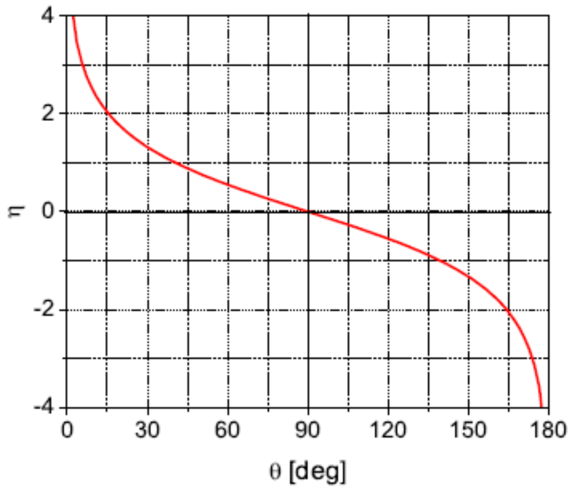

Figure 2.2: Variations of pseudorapidity η with polar angle θ [1].

as the pseudorapidity,

$$y \approx \eta = -\ln\left(\tan\frac{\theta}{2}\right) \tag{2.7}$$

Figure 2.2 shows the variation of pseudorapidity (η) with the polar angle (θ).

2.4 Multiplicity

Multiplicity refers to the total number of particles detected in a collision. Collisions producing a large number of charged particles, correspond to central collisions where the number of nucleon participants is also high. And collisions with the smaller number of produced charged particles correspond to peripheral collisions where the number of nucleon participants is also low. Multiplicity distribution measurements provide idea about the particle-production models. The multiplicity distribution can be used to study the underlying physics of high energy collision experiments. A more detailed discussion [10] on the multiplicity distribution is also given in the next section.

2.5 Transverse energy (E_T)

Transverse energy is one of the global observables to characterize the system formed in heavy-ion collisions at extreme conditions of temperature and energy density. The energy transverse to the beam direction is called transverse energy, which is a multi-particle variable. It can be defined as

$$E_T = \sum_i E_i \sin\theta_i \tag{2.8}$$

$$dE_T(\eta)/d\eta = \sin\theta(\eta) dE(\eta)/d\eta \tag{2.9}$$

The sum is taken over all particles emitted into a fixed solid angle for each event [11].

The energy of an individual particle can be determined by knowing its momenta and particle identification by using a tracking detector and/or the total energy deposited in a calorimeter .

The transverse energy is related to particle multiplicity distribution by the formula

$$\frac{dE_T}{d\eta} \approx < p_T > \frac{dN_{ch}}{d\eta} \tag{2.10}$$

where p_T is the transverse momentum [12].

It is ideal to study transverse energy production to probe the early stage of the heavy-ion collisions because of the following reasons.

a) Before the collision of the two nuclei, the longitudinal phase space is filled with the beam particles only whereas the transverse phase space is empty. But after the collision, particles are produced in all directions hence populating the transverse phase space. Therefore, the energy carried by the particles in the transverse plane has completely emerged from the collision.

b) The initial energy density can be calculated by the Bjorken energy density

formula from the E_T distribution, which is described in the next section.
c) Comparison of this initial energy density calculated in the framework of boost-invariant hydrodynamics from E_T distribution, with that of estimated by the lattice QCD calculations, gives indication of a possible formation of QGP in the heavy-ion collisions.
d) The collision centralities can also be estimated from the minimum bias E_T distribution, the more detailed is described in the next chapter [10].
e) Transverse energy (E_T) production tells about the explosiveness of the interaction.

2.6 Bjorken Energy Density

The main aim of the relativistic heavy-ion collisions is to create the Quark-Gluon Plasma (QGP) and study its properties. So it is important to find the initial energy density including the time evolution of energy density in the overlap region. The initial energy density can be estimated in the central rapidity window by the Bjorken energy density formula, given by:

$$\varepsilon_{Bj}(\tau) = \frac{1}{A_T \tau}\frac{dE_T}{dy}. \tag{2.11}$$

Here A_T is the transverse overlap area of the colliding nuclei, $\frac{dE_T}{dy}$ is the transverse energy density at mid-rapidity and τ is called as the formation time which is generally taken as 1 fm/c. Bjorken energy density becomes ∞, as $\tau \rightarrow 0$. We set the initial formation time as τ_F and can calculate the initially energy density by Bjorken energy density formula at a finite formation time τ_F using E_T, $< m_T >$ and charged particle density of the collisions.

This formula is only valid for a mid-rapidity plateau, which occurs at high collision energies mostly in a baryon-free region and when the duration time (*i.e.* crossing time) is much smaller than the formation time τ_F (i.e $\tau_F >>$

$2R/\gamma$) . Here R is the rest frame radius of the nucleus and γ is the Lorentz [15].

As already mentioned, transverse energy production can be studied to estimate the centrality of the collisions. In the next chapter we proceed to discuss the same.

Chapter 3

Collision Centrality

When two nuclei collide with each other, the impact parameter (which is the perpendicular distance between the two centers of the nuclei) varies from 0 to $R_1 + R_2$, where R_1 and R_2 are the radii of the nuclei. Figure 3.1 shows the schematic representation of collision centrality. For small impact parameter, the collision is called as central collision, where the number of participants nucleon is high and for large impact parameter, the collision is called as peripheral collision, where the number of participants nucleon is low [13].

Experimentally, it is very difficult to calculate the impact parameter and collision centrality. But it is possible to calculate the impact parameter by relating it with the final state particle multiplicity, transverse energy distribution, and also from the number of spectator nucleons. The spectator nucleons are measured by the zero-degree calorimeter (ZDC). From the spectator nucleons, we can calculate the number of participant nucleons by the relation, $N_{part} = N - N_{spectators}$, where N is the total number of nucleons. Particle multiplicity and transverse energy both are proportional to the number of participant nucleons. We can measure the particle multiplicity and transverse energy distribution for minimum-bias collisions. Here high transverse energy (E_T) or high particle multiplicity corresponds to central collision and low transverse energy or low particle multiplicity corresponds to the peripheral collision. Hence collision centrality can

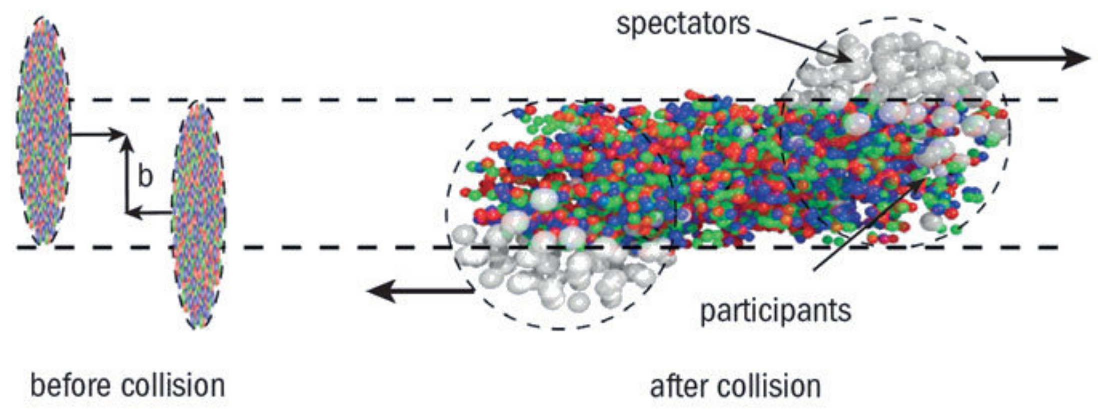

Figure 3.1: A schematic representation of collision centrality (Source : Online).

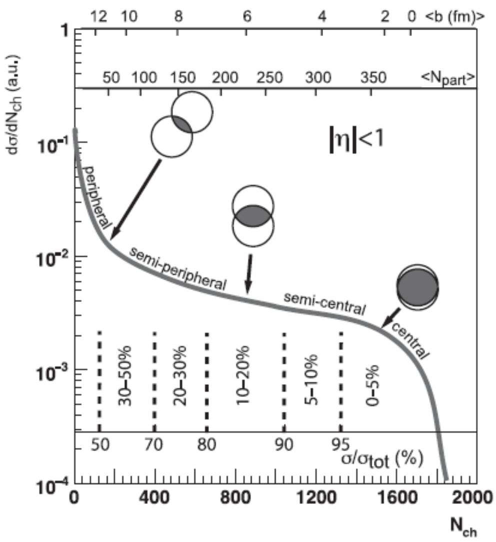

Figure 3.2: A cartoon that shows the definition of centrality [14].

be measured from minimum-bias transverse energy (E_T) or particle multiplicity. Hence the impact parameter can be measured by relating with centrality and the number of spectator nucleons by Glauber type Monte Carlo calculations. In minimum-bias collisions, the collisions having any value of impact parameter ($0 < b < 2R$) are considered. Figure 3.2 shows such an example.

Let us now discuss about some of the basics of gamma distribution, which will be used to describe centrality dependence of E_T-distribution. This we carry out in the next chapter.

Chapter 4

Gamma Distribution

4.1 Introduction

The gamma distribution is a two parameter continuous probability distribution. There are mainly two different parametrizations :
1. With a shape parameter k and a scale parameter θ.
2. With a shape parameter $\alpha = k$ and an inverse scale parameter $\beta = 1/\theta$, called rate parameter.
The gamma probability distribution function with shape-rate parametrizations is

$$f(x;\alpha,\beta) = \frac{\beta(x\beta)^{\alpha-1}exp(-x\beta)}{\Gamma(\alpha)} \tag{4.1}$$

where, α is the shape parameter, β is the scale parameter; $\alpha,\beta > 0$
$\Gamma(\alpha)$ is the gamma function. For positive integers, $\Gamma(\alpha) = (\alpha-1)!$
The mean and variance of gamma probability distribution is given by
mean $(\mu) = \frac{\alpha}{\beta}$ and variance $(\sigma^2) = \frac{\sqrt{\alpha}}{\beta}$.

The behaviour of shape parameter (α) and rate parameter (β) is shown in figures 4.1 and 4.2.

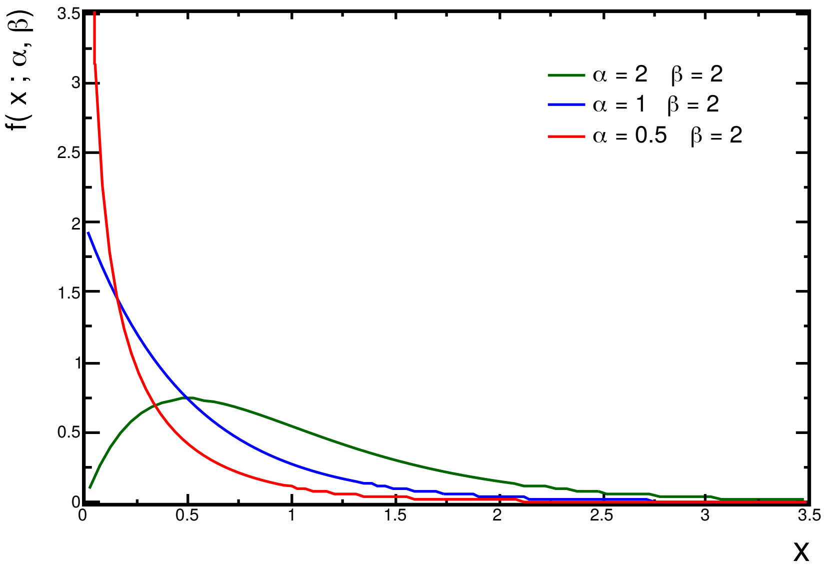

Figure 4.1: Gamma distribution functions at the same value of the rate parameter and different values of the shape parameter.

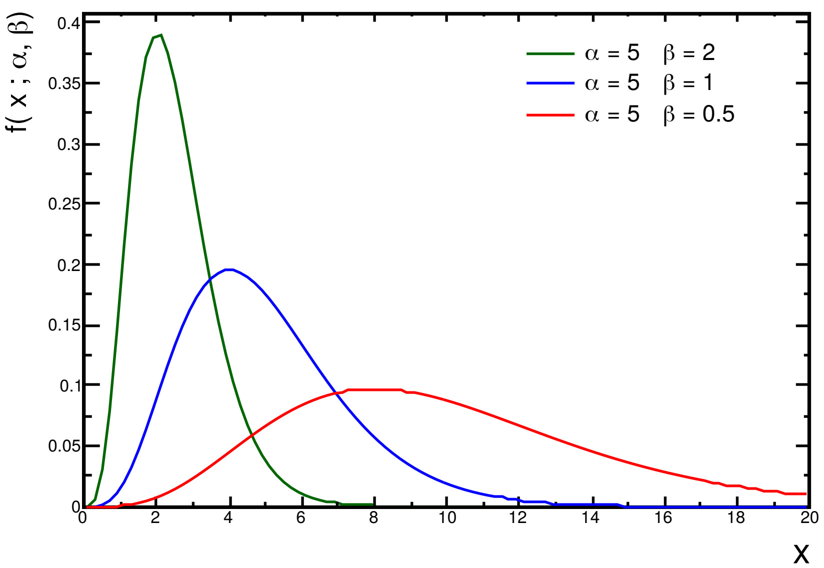

Figure 4.2: Gamma distribution functions at the same value of the shape parameter and different values of the rate parameter.

4.2 Approximation to the convolution of gamma distributions

Let $X_i, i = 1, 2, 3, ...n$ are independently distributed gamma distribution.

$$X_i \sim G(\alpha_i, \beta_i; x_i) = \frac{x_i^{\alpha_i - 1} exp(-x_i/\beta_i)}{\beta_i^{\alpha_i}\Gamma(\alpha_i)} \tag{4.2}$$

$$f(y) = \sum_i^n X_i \tag{4.3}$$

then

$$f(y) \sim G(\rho + k, \beta_{min}; y)$$

where,

$$\rho = \sum_i^n \alpha_i > 0;$$

$$\beta_{min} = min(\beta_i)$$

K is a random variable with prob (K=k)= $\omega_k = Cd_k$, $k = 0, 1, 2, ...$, $d_0 = 1$ And

$$C = \prod_{i=1}^n (\frac{\beta_{min}}{\beta_i})^{\alpha_i}$$

$$d_k = \frac{1}{k} \sum_{i=1}^k i g_i d_{k-i},$$

with

$$g_i = \frac{1}{i} \sum_{j=1}^n \alpha_j (1 - \frac{\beta_{min}}{\beta_j})^i$$

Without loss of generality, we assume $\beta_{min} = \beta_1$,

Therefore, the density of $f(y)$ can be expressed as

$$f(y) = \sum_{k=0}^{k=\infty} \omega_k \frac{y^{\rho+k-1} e^{-y/\beta_1}}{\beta_1^{\rho+k}\Gamma(\rho + k)} \tag{4.4}$$

4.2.1 Case-1 (Convolution of two Gamma distribution functions):

In this case,

$$C = (\frac{\beta_1}{\beta_2})^{\alpha_2}$$

$$g_i = \frac{1}{i}\alpha_2(1-\frac{\beta_1}{\beta_2})^i$$

$$= \frac{1}{i}\alpha_2 p^i, i = 1,2,3,...,$$

where

$$p = (1-\frac{\beta_1}{\beta_2})$$

$$Now, Prob(K=k) = Cd_k = \frac{1}{k!}(\alpha_2)_k(1-p)^{\alpha_2}p^k$$

Where $(\alpha_2)_k$ is the Pochhammer symbol, is given by

$$(\alpha_2)_k = \alpha_2(\alpha_2+1)(\alpha_2+2).....(\alpha_2+k-1) = \frac{(\alpha_2+k-1)!}{(\alpha_2-1)!}$$

Now , $Prob(K=k) = Cd_k$

$$= \frac{1}{k!}\frac{(\alpha_2+k-1)!}{(\alpha_2-1)!}(1-p)^{\alpha_2}p^k$$

$$Cd_k = \binom{k+\alpha_2-1}{k}(1-p)^{\alpha_2}p^k = NB(k;\alpha_2,p) \tag{4.5}$$

, is a negative binomial distribution. Hence the convolution of two Gamma distribution becomes,

$$f(y) = \sum_{k=0}^{k=\infty}\omega_k\frac{y^{\rho+k-1}e^{-y/\beta_1}}{\beta_1^{\rho+k}\Gamma(\rho+k)}$$

$$f(y) = NB(k;\alpha_2,p)G(\rho+k,\beta_1;y) \tag{4.6}$$

4.2.2 Case-2 (n^{th} Convolution of Gamma distribution function):

In this case

$$d_k = \frac{1}{k!}\sum_{i=1}^{k} i g_i d_{k-i}$$

$$= \frac{1}{k!}\sum_{i=1}^{k}(\sum_{j=1}^{n}\alpha_j(1-\frac{\beta_1}{\beta_i})^i)$$

$$= \frac{1}{k!}\sum_{i=1}^{k}\rho p^i$$

$$= \frac{1}{k!}(\rho)_k p^k$$

when the shape parameters α_i's are too small, at that time the approximation becomes very poor. To improve the approximation, a new third parameter p is needed. And w_k becomes a generalized negative binomial distribution with three parameters, defined as

$$GNB(k;r,p,b) = \begin{cases} \frac{\rho}{\rho+bk}\binom{\rho+bk}{k}(1-p)^{\rho+bk-k}p^k & k=0,1,2.... \\ 0 & k \geq \mu, \qquad \rho+b\mu<0; \end{cases} \tag{4.7}$$

for b=1, the generalized negative binomial distribution becomes a negative binomial, and for $0<b<1$, the generalized negative binomial does not exit.

Hence the Convolution becomes ,

$$f(y) = GNB(k;\rho,p,b)G(\rho+k,\beta_1;y) \tag{4.8}$$

In the next chapter all the results of our analysis are discussed.

Chapter 5

Results and Discussion

We have fitted the gamma distribution function (eq. 4.1) to centrality-wise transverse energy distributions for Au+Au collisions at $\sqrt{s_{NN}} = 62.4$ and 200 GeV. The data for this analysis is taken from PHENIX collaboration paper [16] and STAR collaboration paper [17]. In fig. 5.1 a gamma distribution function is fitted to (0-5)% central transverse energy distribution of Au+Au collisions at $\sqrt{s_{NN}} = 62.4$ GeV and the extracted parameters α and β are written below.

$$\alpha = 43.381, \quad \alpha(e) = 0.616$$
$$\beta = 8.276, \quad \beta(e) = 0.060$$

Here, $\alpha(e)$ and $\beta(e)$ denotes the uncertainties in the estimation of the parameters α and β respectively from the fitting. The uncertainties from the fitting are small. From the fig. 5.1, it is clear that transverse energy distribution can be nicely described by a two parameter gamma distribution function (eq. 4.1).

In fig. 5.2, the green coloured curves represent the centrality-wise E_T distributions and the black curve is the minimum-bias curve for Au+Au collisions at $\sqrt{s_{NN}}$ = 62.4 GeV. The convoluted distribution is shown in blue coloured curve whereas the red curve represent the bin-wise summation of the centrality-wise

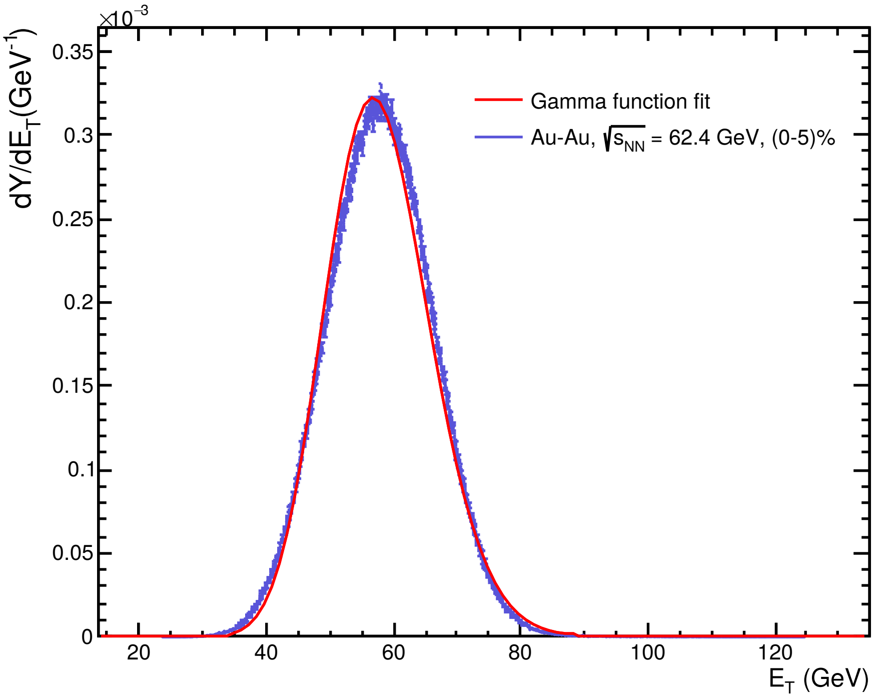

Figure 5.1: Fitting of a Gamma distribution function to (0-5)% central transverse energy distribution for Au+Au collisions at $\sqrt{s_{NN}} = 62.4$ GeV.

curves. Convolution is a mathematical operation, which interacts with two or many input functions and produces a single function as an output. Since the minimum-bias collisions take all the centrality-wise collisions into account, a mathematical convolution of the centrality-wise curves was expected to reproduce the minimum-bias distribution. To check this hypothesis, we convoluted all the centrality-wise E_T distributions to reproduce the minimum-bias curve, but unfortunately, we do not get the desired result. Since the mean of the convoluted curve is the addition of all the means of centrality-wise E_T distribution curves, the convoluted curve shifts towards the right. On the other hand, the bin-wise summation of all the centrality-wise E_T distributions produces the minimum-bias curve as shown by the red coloured curve.

The centrality-wise E_T distributions, corresponding gamma distribution fit functions, minimum-bias curve and the bin-wise summation of the centrality-wise E_T distribution curves for Au+Au collisions at $\sqrt{s_{NN}}$ = 62.4 and $\sqrt{s_{NN}}$ = 200

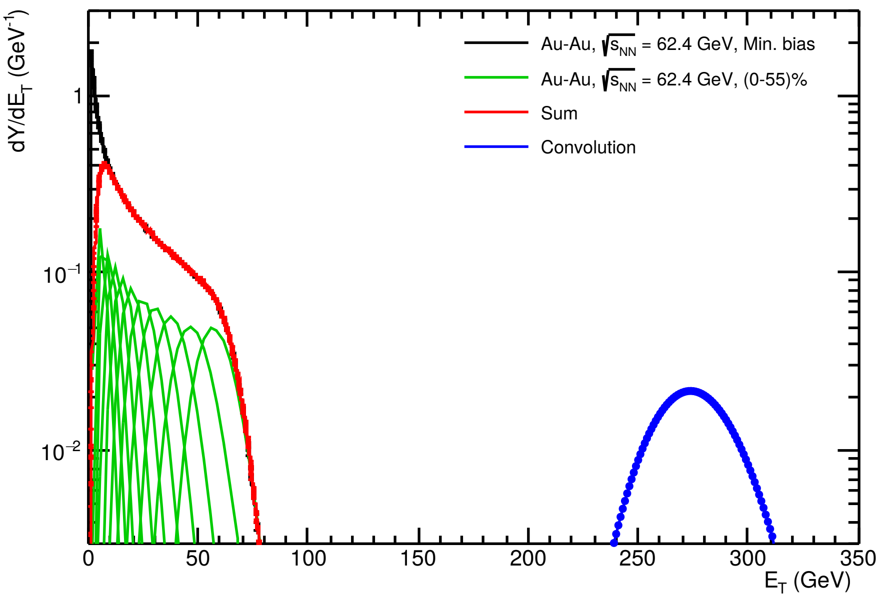

Figure 5.2: Convolution and sum of centrality-wise E_T distributions for Au+Au collisions at $\sqrt{s_{NN}} = 62.4$ GeV.

GeV are shown in fig. 5.3 and fig. 5.4 respectively. As one can see, the summation curve exactly matches with the minimum-bias curve from data for both cases of center-of-mass energy of collisions. The values of the extracted parameters after fitting the gamma distribution function to each of the centrality-wise transverse energy distributions of Au+Au collisions at $\sqrt{s_{NN}}$= 62.4 and $\sqrt{s_{NN}}$ = 200 GeV, are written in table 5.1 and table 5.2 respectively. The extracted parameters α (shape parameter) and β (rate parameter) noted in table 5.1 and table 5.2 are plotted against centrality, which is shown in fig. 5.5 and fig. 5.6 respectively.

Figure 5.5 shows that the shape parameter (α) is centrality dependent but independent of energy. The value of the shape parameter is more for central collisions and becomes less for peripheral collisions. Since in central collisions, more particles are produced, so the transverse energy distribution curve is more symmetric and shape parameter is more. And in peripheral collisions less particles are produced, so the transverse energy distribution curve is less symmetric

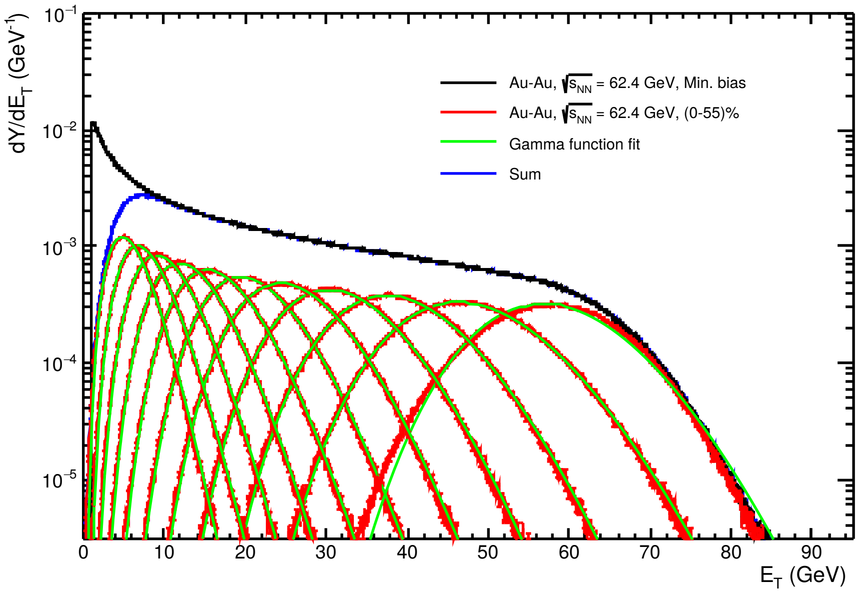

Figure 5.3: Centrality-wise transverse energy distributions for Au+Au collisions at $\sqrt{s_{NN}} = 62.4$ GeV.

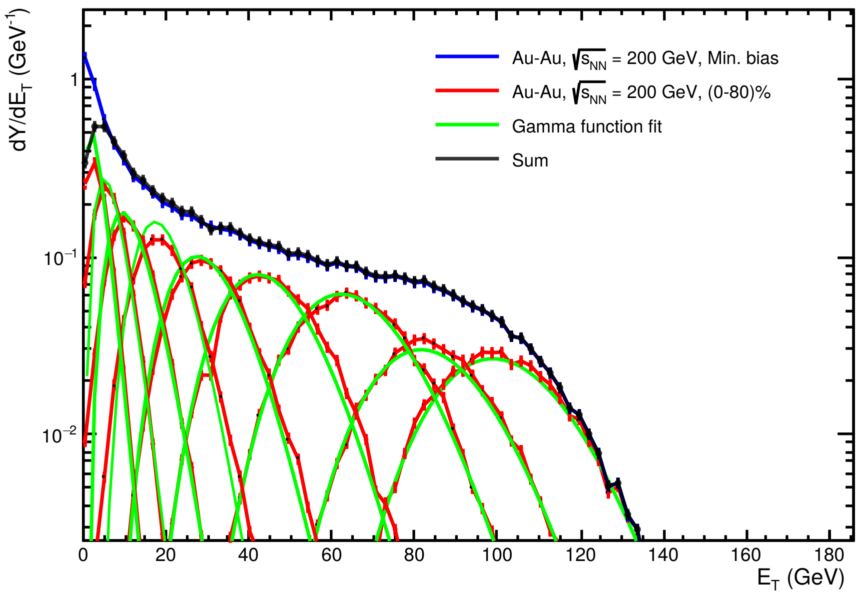

Figure 5.4: Centrality-wise transverse energy distributions for Au+Au collisions at $\sqrt{s_{NN}} = 200$ GeV.

Centrality	α	β	Normalization constant	χ^2/NDF
0%-05%	49.8303	0.860795	0.00657135	13.2225
05%-10%	34.5663	0.725434	0.00668155	1.49976
10%-15%	29.6400	0.765566	0.00667507	1.90562
15%-20%	24.8026	0.786424	0.00667926	1.86309
20%-25%	20.5691	0.803856	0.00668392	1.91201
25%-30%	17.0561	0.826612	0.00668134	2.01292
30%-35%	14.0841	0.855453	0.00668310	2.23491
35%-40%	11.5666	0.891681	0.00668310	2.67953
40%-45%	9.37822	0.931122	0.00668916	3.65557
45%-50%	7.51861	0.977753	0.00668191	5.38846
50%-55%	5.95291	0.803169	0.00666475	10.4639

Table 5.1: Fit results of E_T distributions for Au+Au collisions at $\sqrt{s_{NN}} = 62.4$ GeV.

Centrality	α	β	Normalization constant	χ^2/NDF
0%-05%	48.2946	0.478431	18571.3	10.9661
05%-10%	43.8709	0.522836	18940.1	8.92791
10%-20%	25.1522	0.38315	35202.8	9.90973
20%-30%	18.7188	0.409616	37020.8	8.7833
30%-40%	13.3436	0.433682	35515.6	10.9293
40%-50%	10.3071	0.456527	35869.2	9.9223
50%-60%	5.48672	0.452796	35819.4	11.5936
60%-70%	3.34994	0.474283	38728.9	10.065
70%-80%	1.69271	0.44344	38007.9	9.25383

Table 5.2: Fit results of E_T distributions for Au+Au collisions at $\sqrt{s_{NN}} = 200$ GeV.

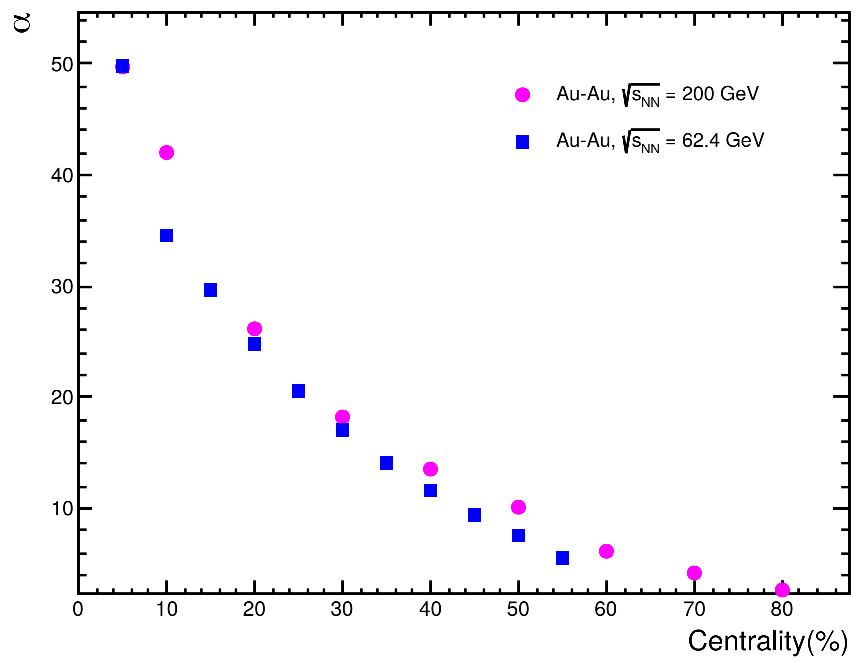

Figure 5.5: Variation of α with centrality for Au+Au collisions at $\sqrt{s_{NN}} = 62.4$ and 200 GeV.

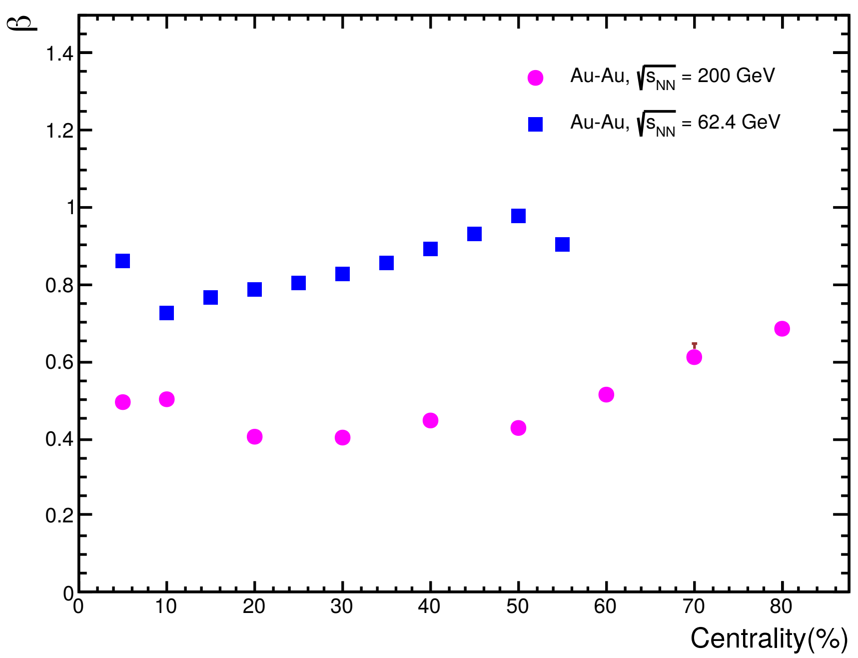

Figure 5.6: Variation of β with centrality for Au+Au collisions at $\sqrt{s_{NN}} = 62.4$ and 200 GeV.

and shape parameter is less. Figure 5.6 shows that the rate parameter (β) is energy dependent but shows a little variation as a function of centrality.

5.1 Summary and Conclusions

To understand the paramount dependence of transverse energy production, we have fitted a gamma distribution to the centrality-wise E_T distribution for Au+Au collisions at $\sqrt{s_{NN}}$ = 62.4 GeV and $\sqrt{s_{NN}}$ = 200 GeV and we get the following results.

1. The sum of all the centrality-wise transverse energy distributions gives the minimum bias distribution.
2. The shape parameter (α) is centrality dependent and energy independent.
3. The shape parameter is more for central collisions owing to the symmetrical shape of the distribution and decreases towards the peripheral collisions.
4. The rate parameter (β) is energy dependent but shows a little variation as one moves from central to peripheral collisions.

Bibliography

[1] R. Sahoo, [arXiv:1604.02651 [nucl-ex]].

[2] J.D. Bjorken, Phys. Rev. D **27**, 140-151 (1983) doi:10.1103/PhysRevD.27.140

[3] F. Karsch, Lect. Notes Phys. **583**, 209-249 (2002) doi:10.1007/3-540-45792-5_6 [arXiv:hep-lat/0106019 [hep-lat]].

[4] S. Borsanyi, G. Endrodi, Z. Fodor, A. Jakovac, S.D. Katz, S. Krieg, C. Ratti and K.K. Szabo, JHEP **11**, 077 (2010) doi:10.1007/JHEP11(2010)077 [arXiv:1007.2580 [hep-lat]].

[5] N. Armesto, J. Phys. G **35**, 104042 (2008) doi:10.1088/0954-3899/35/10/104042 [arXiv:0804.4158 [hep-ph]].

[6] R.S. Bhalerao, doi:10.5170/CERN-2014-001.219 [arXiv:1404.3294 [nucl-th]].

[7] R. Sahoo, AAPPS Bull.**29**,16-21(2019) doi:10.22661/AAPPSBL.2019.29.4.16 [arXiv:1908.10566 [nucl-ex]].

[8] S. Borsanyi, Z. Fodor, C. Hoelbling, S. D. Katz, S. Krieg and K. K. Szabo, Phys. Lett. B **730**, 99-104 (2014) doi:10.1016/j.physletb.2014.01.007 [arXiv:1309.5258 [hep-lat]].

[9] T. Abbott, L. Ahle, Y. Akiba, D. Alburger, D. Beavis, L. Birstein, M. A. Bloomer, P. D. Bond, H. C. Britt and B. Budick, *et al.* Phys. Rev. C **63**, 064602 (2001) [erratum: Phys. Rev. C **64**, 029901 (2001)] doi:10.1103/PhysRevC.63.064602.

[10] R. Sahoo, A. N. Mishra, N. K. Behera and B. K. Nandi, Adv. High Energy Phys. **2015**, 612390 (2015) [erratum: Adv. High Energy Phys. **2017**, 4517153 (2017)] doi:10.1155/2015/612390 [arXiv:1408.5773 [nucl-ex]].

[11] K. Adcox *et al.* [PHENIX], Phys. Rev. Lett. **88**, 022301 (2002) doi:10.1103/PhysRevLett.88.022301 [arXiv:nucl-ex/0109003 [nucl-ex]].

[12] S. S. Adler *et al.* [PHENIX], Phys. Rev. C **71**, 034908 (2005) [erratum: Phys. Rev. C **71**, 049901 (2005)] doi:10.1103/PhysRevC.71.034908 [arXiv:nucl-ex/0409015 [nucl-ex]].

[13] CERN Cour. **53N4**, 31-33 (2013).

[14] L. Kluberg and H. Satz, doi:10.1007/978-3-642-01539-7_13 [arXiv:0901.3831 [hep-ph]].

[15] Z.W. Lin, Phys. Rev. C **98**,034908 (2018) doi:10.1103/PhysRevC.98.034908 [arXiv:1704.08418 [nucl-th]].

[16] S. S. Adler *et al.* [PHENIX], Phys. Rev. C **89**, no.4, 044905 (2014) doi:10.1103/PhysRevC.89.044905 [arXiv:1312.6676 [nucl-ex]].

[17] J. Adams *et al.* [STAR], Phys. Rev. C **70**, 054907 (2004) doi:10.1103/PhysRevC.70.054907 [arXiv:nucl-ex/0407003 [nucl-ex]].